Research Paper

Localization and Differential Activity of P-glycoprotein in the Bovine Olfactory and Nasal Respiratory Mucosae

Karunya K. Kandimalla[1,2] and Maureen D. Donovan[1,3]

Purpose. The purpose of this study was to demonstrate that P-glycoprotein (P-gp) is localized in the olfactory mucosa and is capable of limiting the nose-to-brain transport of substrates. Bovine olfactory and nasal respiratory mucosae were compared to both localize P-gp and to measure its activity within the epithelia.

Methods. Immunolocalization was performed on the bovine olfactory and nasal respiratory mucosa using the C219 monoclonal antibody. Flux of etoposide, a substrate reported to be primarily effluxed by P-gp, across bovine olfactory and nasal respiratory mucosae was measured using Sweetana-Grass (Navicyte®) vertical diffusion cells. Experiments were performed to evaluate the effect of directionality, donor concentration, and the presence of inhibitors.

Results. Dense staining was observed on the apical surface of the ciliated epithelial cells and within the submucosal lymphatics/vasculature and mucosal glands of the bovine olfactory and nasal respiratory mucosae. Staining in the nasal respiratory epithelium was weak and patchy when compared to that observed in the olfactory mucosa. The secretory transport (J_{s-m}) kinetics of etoposide in the olfactory ($K_m = 260.5$ μM, $V_{max} = 0.179$ μM/cm^2 min) and nasal respiratory ($K_m = 46.9$ μM, $V_{max} = 0.034$ μM/cm^2 min) mucosae were observed to be saturable and concentration-dependent. The flux of etoposide in the submucosal–mucosal (J_{s-m}) direction was significantly greater than the flux in the mucosal–submucosal (J_{m-s}) direction in both the olfactory and nasal respiratory mucosa. The efflux ratios (J_{s-m}/J_{m-s}) of etoposide across the olfactory and the nasal respiratory mucosae were 2.02 and 2.10, respectively. In the presence of inhibitors such as 2,4-dinitrophenol (1 mM) and quinidine (1 mM), etoposide showed an increase in J_{m-s} and a decrease in J_{s-m}. The etoposide efflux was unaffected in the presence of a specific multiresistance associated protein 1 (MRP1) inhibitor (MK571) and methotrexate, a substrate for BCRP and MRP1–4.

Conclusions. P-gp was localized in the epithelial cells, nasal glands, and the vascular endothelium of both the bovine olfactory and nasal respiratory mucosae, and the expressed P-gp was capable of effluxing a substrate such as etoposide. The K_m and V_{max} of etoposide efflux were higher in the olfactory mucosa compared to the nasal respiratory mucosa, and the expression of P-gp seems to be greater in the olfactory epithelium compared to the nasal respiratory epithelium based on the staining density observed using immunohistochemistry.

KEY WORDS: CNS; efflux; etoposide; membrane transport proteins; nasal respiratory mucosa; nose–brain transport; olfactory mucosa; P-glycoprotein.

INTRODUCTION

Delivery of drugs to the central nervous system (CNS) via the nasal cavity provides the potential to circumvent the blood–brain barrier (BBB). Hydrophilic compounds such as dopamine (1) and cephalexin (2), both of which are unable to permeate the BBB, have been shown to access the CNS via the nasal cavity. The nasal administration of lipophilic compounds such as progesterone (3) and midazolam (4), which are able to penetrate the BBB, also resulted in higher C_{max} and shorter t_{max} values in the cerebrospinal fluid (CSF) than following intravenous administration. Delivery of large proteins such as nerve growth factor (NGF) to the brain has also been demonstrated via a connection between the nose and brain (5).

Several tracer studies have shown the existence of a direct connection between the cranial CSF and the olfactory mucosa through which low molecular weight drugs and therapeutic peptides can access the CNS. In an attempt to study the role of the olfactory pathway in CSF drainage, Erlich and coworkers (6) observed that ferritin moved into the olfactory submucosa 12 min after injection into the lateral

[1] College of Pharmacy, The University of Iowa, Iowa City, Iowa 52242, USA.

[2] Present address: College of Pharmacy and Pharmaceutical Sciences, Florida A&M University, Tallahassee, Florida 32307, USA.

[3] To whom correspondence should be addressed. (e-mail: Maureen-donovan@uiowa.edu)

ventricles of rats. Four hours after the injection, the quantity of ferritin in the olfactory submucosa was increased, but the distribution pattern remained unchanged. In a similar study, Kida *et al.* (7) found that Indian ink particles present in the subarachnoid space drained directly into discrete channels that passed through the cribriform plate and into the lymphatics in the olfactory submucosa. Both of these studies also indicated that the tracers did not completely permeate through the olfactory epithelium and did not appear within the nasal cavity. Although the tracers used in these studies were large in size, it is reasonable to assume that the olfactory epithelium acts as a barrier to the transport of small molecules as well as macromolecules between the nasal cavity and the CNS in the mucosal–submucosal (m–s) or submucosal to mucosal (s–m) directions.

The olfactory region consists of the olfactory mucosa lining the cribriform plate of the ethmoid bone that separates the nasal and cranial cavities. The olfactory epithelium overlies a thick connective tissue (lamina propria) that contains blood vessels, olfactory nerve bundles, and nasal glands. The olfactory epithelium is a pseudostratified columnar epithelium composed of three types of cells: olfactory neurons, sustentacular (supporting) cells, and basal cells. It has been proposed that macromolecular complexes such as wheat germ agglutinin–horseradish peroxidase (8) and metals such as cadmium and manganese (9) are taken up by the olfactory neurons and transported to the olfactory bulb very slowly by an axonal pathway (10). However, the transport of low molecular weight drugs (11,12) and some macromolecules (13) from the nasal cavity to the CSF is very rapid. Hence, it is believed that these molecules permeate through the olfactory epithelium to reach the CSF via the perineuronal spaces and olfactory submucosal lymphatics rather than via the axonal pathway.

Chou and Donovan (11) reported that model antihistamine compounds sharing similar physicochemical properties exhibited different CNS distribution patterns in rats following nasal administration. Hydroxyzine and triprolidine readily reached the CNS, whereas no measurable amounts of chlorcyclizine or chlorpheniramine were observed. The lack of predictive CNS distribution based on physicochemical properties prompted the investigation of specialized transport systems that could prevent molecules from permeating through the olfactory mucosa. One important transport system in many mucosal and epithelial tissues is P-glycoprotein (14), which has been shown to be capable of effluxing many diverse substrates (15).

P-glycoprotein is a member of the ATP-binding cassette (ABC) superfamily of proteins that was first implicated in multidrug resistance due to its ability to efflux a variety of anticancer drugs such as etoposide from malignant cells (16). P-gp has been reported to be localized in the cells of tissues that have specific barrier functions, i.e., blood–brain barrier, blood–placental barrier, blood–testis barrier, blood–nerve barrier, and the intestinal mucosa (17). On a cellular level, P-gp is frequently localized in the plasma membrane and is believed to be responsible for removing agents that partition into the membrane (18).

Because the olfactory and nasal respiratory mucosae are the primary barriers to drug absorption from the nasal cavity, an understanding of the location and activity of transporters such as P-gp in both mucosae is essential to understanding the role of efflux in nose-to-brain transport. Wioland *et al.* (19) reported that efflux transporters such as P-gp and multiresistance associated protein (MRP) 1 and 2 were expressed in the epithelium and nasal glands of the human nasal respiratory mucosa. Studies conducted by Graff and Pollack (20,21) demonstrated that P-gp was present in the murine olfactory mucosa and limited the brain uptake of substrates after intranasal administration. We have demonstrated that chlorpheniramine and chlorcyclizine are effluxed across the bovine olfactory mucosa by transporters such as P-gp (22). The objective of this study was to localize P-gp in the bovine olfactory mucosa, determine its functionality using etoposide as a substrate, and compare the results to those observed in the bovine nasal respiratory mucosa.

MATERIALS AND METHODS

Chemicals and Reagents

Monoclonal anti P-glycoprotein antibody (C219) and DAKO EnVision™ system were purchased from Dako Corporation (Carpinteria, CA, USA). Etoposide, quinidine HCl, 2, 4-dinitrophenol (2,4-DNP), dimethyl sulfoxide (DMSO), methotrexate (MTX), and minimum essential Eagle's medium with Earl's salts (MEM) were obtained from Sigma (St. Louis, MO, USA). MK 571 was obtained from CalBiochem (CalBiochem, La Jolla, CA, USA). Kreb's Ringer buffer (KRB) salts and HPLC solvents were obtained from Fisher Scientific (Chicago, IL, USA).

Kreb's Ringer Buffer

Kreb's Ringer Buffer was prepared by adding 0.5 mM $MgCl_2$, 4.56 mM KCl, 119 mM NaCl, 0.7 mM Na_2HPO_4, 1.3 mM NaH_2PO_4, 10 mM D-Glucose, 2.5 mM $CaCl_2$, and 15 mM $NaHCO_3$ to deionized water. The pH was adjusted to 6.5 ± 0.2 with either 1 N HCl or NaOH.

Nasal Mucosal Samples

Bovine olfactory and nasal respiratory mucosae were obtained from the Roherkassee Meat Co. (Williamsburg, IA, USA). After the animals were decapitated, longitudinal incisions along the lateral walls of the nasal cavity and a vertical incision along the ocular plane were made to expose the nasal respiratory and olfactory regions of the bovine nasal cavity. Full-thickness olfactory and nasal respiratory mucosae were harvested from the ethmoid and maxilloturbinates, respectively. The tissues used for immunohistochemistry were rinsed thoroughly with MEM, flash frozen in isopentane cooled by liquid nitrogen, and transported to the microscopy facility for further processing. The tissues used in the transport studies were rinsed thoroughly with KRB and stored in fresh KRB maintained on ice. Transport studies were conducted within 4 h of the procurement time. The mucosal tissues were determined to be viable after the transport studies using one of several methods including: (1) live-and-dead cell assay (LIVE/DEAD® viability/cytotoxicity kit; Molecular Probes, Eugene, OR); (2) measurement of the

flux of a well-characterized paracellular marker (Lucifer yellow) across the mucosal tissue; (3) measurement of the electrical resistance across the mucosal membrane (EVOM, World Precision Instruments, Sarasota, FL), USA.

Immunolocalization of P-Glycoprotein

Antibodies

Primary antibody (anti-P-glycoprotein antibody, C219) is an antihuman mouse IgG_{2a} monoclonal antibody that recognizes an intracellular epitope located on the carboxy terminal portion of P-gp (23,24). The secondary antibody was labeled with horseradish peroxidase (HRP). Negative controls were performed by replacing the primary antibody with an irrelevant IgG_{2a} of the same origin. The secondary antibody and the isotype matched negative control were components of the DAKO EnVision™ system.

Immunohistochemistry

The frozen tissues were cut into 10-μm sections using a Microm HM505E cryostat (Richard Allen, Inc., Richland, MI, USA). The sections were mounted on Superfrost PLUS slides (Fisher Scientific), fixed by using a mixture of 75% acetone and 25% ethanol for 5 min at room temperature, and air-dried overnight at −20°C. The sections were washed with distilled water followed by PBS (pH = 7.1) to remove the cryomounting medium. Dako quenching solution (a component of the DAKO EnVision™ system) was used to block the sections against endogenous peroxidase. The sections were rinsed with PBS and incubated with blocking solution containing 10% normal goat serum + 1% bovine serum albumin for approximately 20 min.

The sections were subsequently incubated at 4°C for 48 h with primary antibody diluted (1:2) with 1% fetal calf serum in PBS followed by incubation with the secondary antibody (DAKO EnVision™ System) for 30 min. After rinsing thoroughly with PBS followed by distilled water, the sections were exposed to a solution containing diaminobenzidine chromogen (DAKO EnVision™ System) for 5 min. The sections were rinsed with running tap water for 15 min and counterstained with methyl green.

Etoposide Permeability

The permeation of etoposide across the bovine olfactory and nasal respiratory mucosae was measured using Sweetana-Grass (Navicyte®) vertical diffusion cells. The temperature was maintained at 37 ± 0.5°C using a circulating water bath. The mucosal tissue was mounted between the donor and receiver compartments and equilibrated for 30 min in KRB at pH 6.5 ± 0.2. After equilibration, the KRB was replaced with 1 ml each of the donor (etoposide + 0.1% DMSO in KRB) and the receiver solutions (0.1% DMSO in KRB). The donor and the receiver chambers were kept under a constant carbogen flow (95% O_2 + 5% CO_2) at the rate of 3–4 bubbles/s. Samples (200 μl) were taken from the receiver solution at regular time intervals for up to 120 min and analyzed for the presence of etoposide. The solution removed was replaced with fresh, prewarmed receiver solution.

Concentration Dependence and Directionality of Etoposide Transport

Etoposide flux across the bovine olfactory and nasal respiratory mucosae was determined in the mucosal–submucosal (m–s) direction by mounting the tissue so that the epithelial surface was in contact with the donor solution. In a similar fashion for the s–m studies, the submucosal surface of the mucosa was in contact with the donor solution. The effect of donor concentration on the submucosal–mucosal (s–m) flux of etoposide across the bovine olfactory and nasal respiratory mucosae was investigated at concentrations ranging from 21 to 425 μM. To compare the magnitude of s–m and m–s flux, two concentrations of etoposide were selected. The s–m and m–s flux across nasal respiratory mucosa was measured using a 42-μM etoposide concentration in the donor chamber. A concentration of 212 μM was used when comparing the directional flux in the olfactory mucosa.

Inhibition Studies

Etoposide flux in both the mucosal–submucosal and submucosal–mucosal directions was measured in the presence of quinidine (1 mM) (25), 2,4-DNP (1 mM) (25), MK571 (25 μM) (26,27), or methotrexate (1 mM) (28). For all inhibition studies, the tissues were preequilibrated with the inhibitor solution (inhibitor + 0.1% DMSO in KRB) in the donor and receiver chambers for 30 min at 37 ± 0.5°C. At the start of the experiment, the donor chamber was filled with 1 ml of inhibitor solution containing etoposide and the receiver chamber was filled with 1 ml of inhibitor solution. The pH of the inhibitor-containing donor and receiver solutions (except for methotrexate) was maintained at 6.4 ± 0.2. The pH of the donor and receiver solutions containing methotrexate was maintained at 7.4 ± 0.2 due to the low solubility of methotrexate at pH 6.4. The donor concentrations of etoposide used for studies with nasal respiratory mucosa and olfactory mucosa were 42 and 212 μM, respectively.

HPLC Analysis

Analysis of etoposide was carried out with an HPLC system consisting of a Hitachi L-6200 Intelligent pump and L-4000 UV detector set at 230 nm (Hitachi, San Jose, CA, USA), Shimadzu CR-501 Chromatopac Integrator (Shimadzu, Columbia, MD, USA) and Waters 712 WISP autosampler (Waters Corp., Milford, MA). A Luna C8 (2) column (5 μm; 250 × 4.60 mm; Phenomenex, Torrance, CA, USA) and a mobile phase of 40% acetonitrile, 1% glacial acetic acid, and 59% water pumped at 1 ml/min were used.

Data Analysis

Flux of etoposide across the olfactory or nasal respiratory mucosa in either the mucosal–submucosal ($J_{m–s}$) or submucosal–mucosal ($J_{s–m}$) direction was calculated from the linear portion of the cumulative mass transported vs. time

profile using Fick's first law. The ratio of J_{s-m}/J_{m-s} was denoted as the efflux ratio (ER). The concentration dependence of flux was quantified by fitting the following Michaelis–Menten-type expression (25) to the data using GraphPad Prism version 3.03 (GraphPad Software, San Diego, CA, USA).

$$J_{s-m} = [(J_{max} \times C)/(K_m + C)] + P \times C \qquad (1)$$

where J_{max} is the maximal rate of s–m flux, C is the donor concentration, K_m is the Michaelis–Menten constant, and P is the passive permeability.

Results from the flux experiments are presented as mean values ± standard deviation. A Student's t test or one-way ANOVA followed by Tukey's multiple comparison tests was performed to compare the means. A value of $p < 0.05$ was considered statistically significant.

RESULTS

Immunolocalization of P-gp in Bovine Olfactory and Nasal Respiratory Mucosae

At low magnification, dense staining was observed in the olfactory epithelium (Fig. 1a). The boxed region of Fig. 1a at higher magnification (Fig. 1b) highlights the staining on the apical surface of the ciliated olfactory epithelial cells. Intense
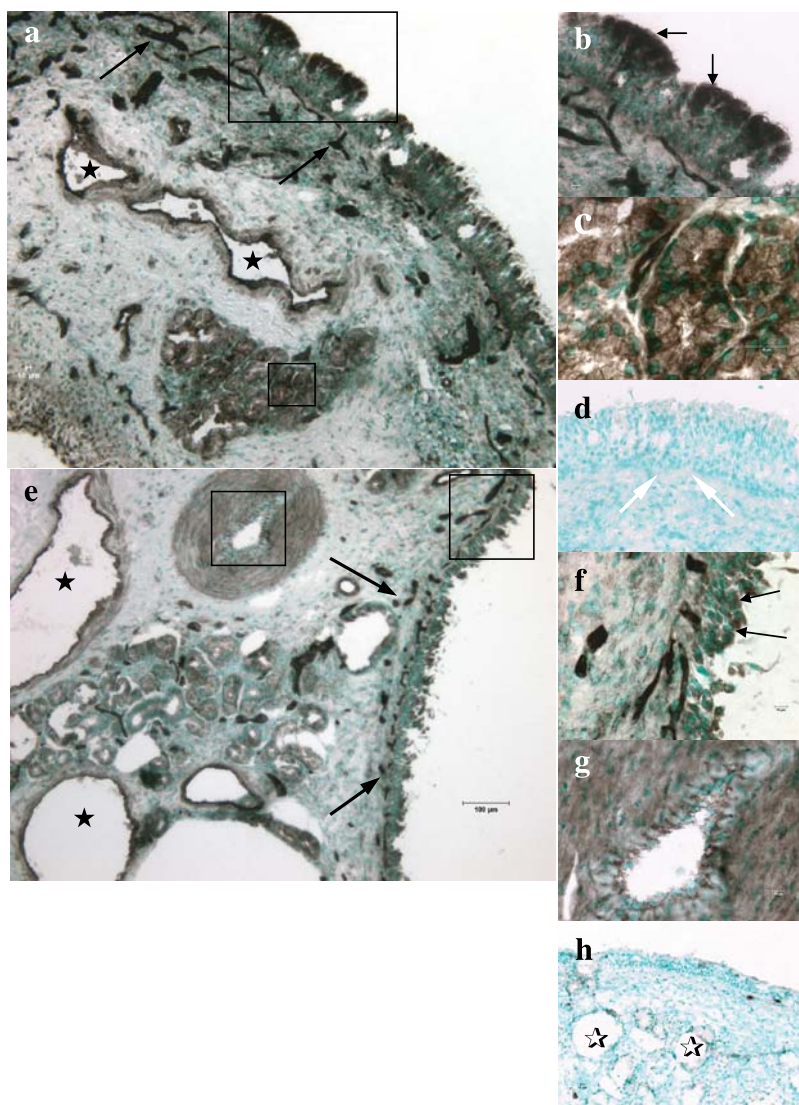

Fig. 1. Immunolocalization of P-glycoprotein (P-gp) (C219 antibody) in bovine olfactory and nasal respiratory mucosae. Dark-stained region represents C219 and P-gp reaction product, (a) olfactory mucosa (20×), (b) boxed epithelial region of (a) at (40×), (c) boxed glandular region of (a) at (100×), (d) control olfactory tissue, (e) nasal respiratory mucosa at (20×), (f) boxed epithelial region of (e), (g) endothelial cells lining the vascular lumen, and (h) control nasal respiratory tissue. ★ Localization of P-gp in the submucosal vascular spaces. ☆ Absence of P-gp in the submucosal vascular spaces of the control. Filled arrows indicate the localization of P-gp and the open arrows indicate the absence of P-gp in the controls.
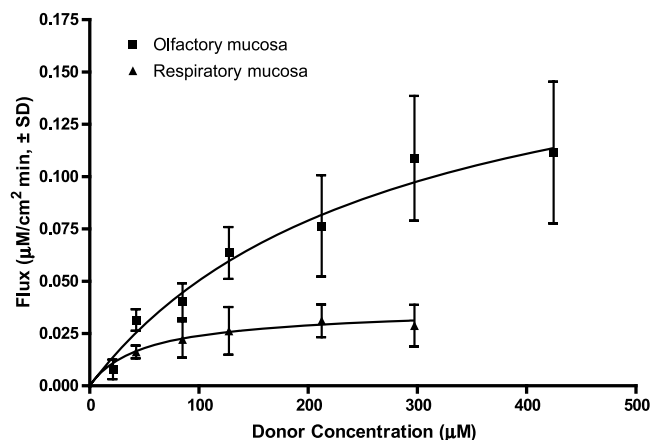
Fig. 2. Concentration dependence of submucosal to mucosal flux of etoposide across bovine olfactory and respiratory mucosae at pH 6.5 ± 0.2. Data points represent the mean flux $\pm$ SD ($n = 3$–6).

staining was also observed in the submucosal lymphatics, in the capillary endothelium of the vascular spaces, and in the nasal glands within the submucosa. Intracytoplasmic staining within the glands was faint and granular (Fig. 1c). No staining was observed in the epithelium, submucosal lymphatics, nasal glands, or other submucosal structures of the control olfactory sections treated with the irrelevant IgG$_{2a}$ (Fig. 1d).

Similar staining patterns were also observed in the nasal respiratory epithelium (Fig. 1e). However, the intensity of staining was weak and patchy when compared to the olfactory mucosa (Fig. 1f). The submucosal lymphatics and vasculature of the respiratory mucosa were densely stained and endothelial staining of the large blood vessels was apparent. Homogeneous staining was observed in the vascular smooth muscle surrounding the large arteries of the nasal submucosa, potentially due to the reported cross reactivity of C219 with the heavy chain of myosin present in smooth muscle (29). No consistent staining was observed in the endothelium of the arterial lumen (Fig. 1g). These large capillaries were not observed in the olfactory mucosal sections, probably due to the lower vascularity of the olfactory mucosa compared to the nasal respiratory mucosa. The cell membranes of the nasal glands in the nasal

respiratory submucosa were densely stained, whereas the intracellular staining was weak and granular. No staining by C219 was observed in any of the epithelial or submucosal structures in the control nasal respiratory tissue (Fig. 1h).

Etoposide Permeability

Concentration Dependence

The secretory (submucosal–mucosal) transport kinetics of etoposide in the olfactory and respiratory mucosae were observed to be saturable and concentration-dependent (Fig. 2). The K_m, V_{max}, and permeability (P) parameters of etoposide efflux across the olfactory mucosa obtained by fitting Eq. (1) to the s–m flux (J_{s-m}) vs. donor concentration results were found to be 260.5 μM, 0.179 μM/cm^2 min, and 6.5×10^{-6} cm/min, respectively. The K_m, V_{max}, and P for etoposide in the respiratory mucosa, obtained in a similar fashion, were found to be 46.9 μM, 0.034 μM/cm^2 min, and 5.0×10^{-6} cm/min, respectively.

Directionality

To investigate the presence of carrier-mediated transport, the directionality of etoposide flux across the bovine olfactory and respiratory mucosae was determined. In the case of the olfactory mucosa, the J_{s-m} of etoposide was significantly greater than the J_{m-s} (Fig. 3a) with an efflux ratio (ER = J_{s-m}/J_{m-s}) of 2.02. In the nasal respiratory mucosa, the J_{s-m} was also significantly greater than the J_{m-s} with an efflux ratio of 2.1. The donor concentration used in the studies with the respiratory mucosa was 42 μM rather than 212 μM as in the olfactory mucosa, because the etoposide efflux in the respiratory mucosa was saturated at donor concentrations greater than 80 μM (Fig. 2).

Inhibition Studies

The J_{m-s} and J_{s-m} of etoposide (212 μM) in the presence of 1 mM 2,4-DNP (metabolic inhibitor); 1 mM quinidine (a mixed inhibitor of P-gp and MRP 1 and 2 (26), 25 μM MK571 (specific MRP1 inhibitor) (26), or 1 mM methotrexate (a
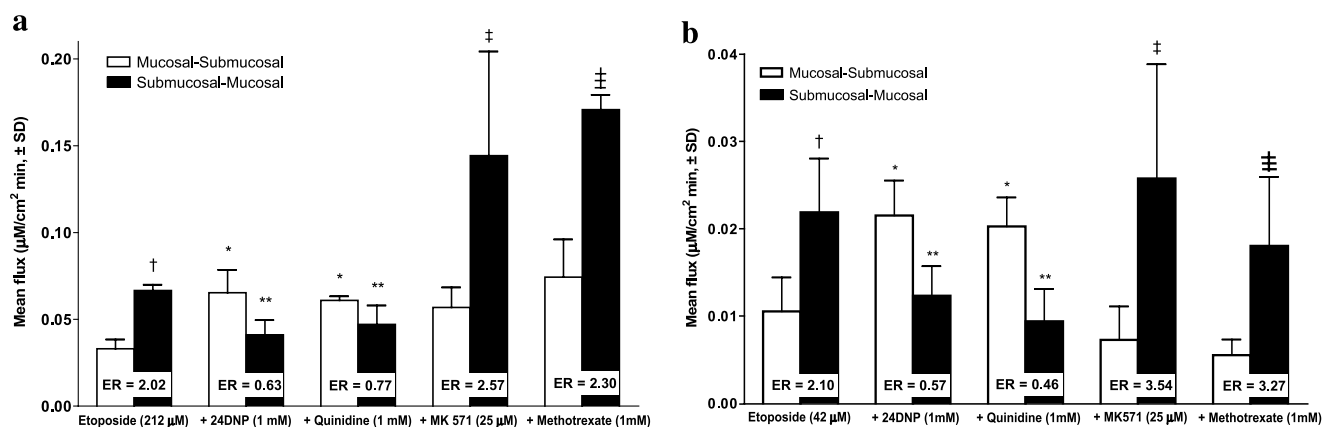

Fig. 3. Effect of inhibitors on the polarized transport of etoposide at pH 6.5 ± 0.2 or 7.4 ± 0.2 (for methotrexate) across (a) bovine olfactory mucosa (control = 212 μM etoposide) (b) bovine nasal respiratory mucosa (control = 42 μM etoposide). Efflux ratio (ER) = J_{s-m}/J_{m-s}; †J_{m-s} (control) $< J_{s-m}$ (control); ⋆$J_{m-s} > J_{m-s}$ (control); ⋆⋆$J_{s-m} < J_{s-m}$ (control); ‡J_{m-s} (MK571) $< J_{s-m}$ (MK571), ⫲J_{m-s} (Methotrexate) $< J_{s-m}$ (Methotrexate); $n = 3$–6.

substrate of MRP1–4 and BCRP) (28, 30–33) were investigated in the bovine olfactory mucosa. Similar studies were also conducted in the nasal respiratory mucosa, but with a lower donor concentration of etoposide (42 μM). One-way ANOVA followed by Tukey's multiple comparison testing showed that, in the presence of 2,4-DNP or quinidine, the J_{s-m} of etoposide across the olfactory (Fig. 3a) or the nasal respiratory (Fig. 3b) mucosae decreased significantly compared to the J_{s-m} of the noninhibited s–m etoposide flux. The J_{m-s} of etoposide across the olfactory (Fig. 3a) or the nasal respiratory (Fig. 3b) mucosa increased significantly compared to the noninhibited m–s etoposide flux (control). The magnitude of change in J_{m-s} and J_{s-m} of etoposide was nearly identical in the presence of either 2,4-DNP or quinidine and the efflux ratio in both olfactory and respiratory mucosae was reduced to less than 1 in the presence of these inhibitors. In the presence of MK571, however, the J_{s-m} of etoposide across the olfactory (Fig. 3a) and the nasal respiratory (Fig. 3b) mucosae remained significantly greater than the J_{m-s} with efflux ratios of 2.57 and 3.54, respectively. Similarly, in the presence of methotrexate the J_{s-m} of etoposide across the olfactory (Fig. 3a) and the nasal respiratory (Fig. 3b) mucosae was significantly greater than the J_{m-s} with efflux ratios 2.3 and 3.27, respectively.

DISCUSSION

Because the olfactory and respiratory epithelia are the primary barriers to drug absorption from the nasal cavity, the localization and activity of P-gp within these barriers has a significant impact on the understanding of nasal bioavailability. The apical location of P-gp restricts the transcellular absorption of P-gp substrates. For substrates that have reached the olfactory submucosa, absorption into the blood or CSF is further restricted by the P-gp located in the endothelium of the vascular spaces and submucosal lymphatics.

The morphology of the bovine and human respiratory and olfactory mucosa has been well characterized by previous investigators (34–36). Their results show that the epithelial cells, sustentacular cells, neurons, tight junctions, and the pattern of intercellular arrangements have remarkable interspecies consistency. Excised bovine nasal mucosa has been validated as an *in vitro* model to study drug transport and metabolic pathways in the nasal epithelium (37). Other investigators have also utilized excised bovine olfactory mucosa as a source for cells and subcellular fractions to study olfactory mucosal metabolism (38,39). Additional studies have been conducted to compare the permeability of numerous other model compounds across bovine olfactory and respiratory mucosae. These studies have demonstrated that, when adjusted for thickness differences, there are no substantial differences in the passive permeabilities of various compounds across either of these mucosal tissues (35). However, the differential expression of various influx and efflux transporters in the olfactory and respiratory mucosae has been observed. These differences have been shown to affect the overall permeability of selected substrates across these mucosae (22). The immunostaining of the bovine respiratory mucosa showed similarities with that of the human respiratory mucosa with the exception that the human respiratory

mucosa showed intense staining along the circumference of the basal cells, except at points of contact with the basal lamina; this was not observed in the bovine respiratory mucosa (19). This localization of P-gp in the basal cells, in addition to at the apical surface, would enhance the epithelial barrier properties against potentially toxic inhaled substances.

Etoposide was effluxed from the bovine olfactory and respiratory mucosae demonstrated by the high efflux ratios (Fig. 3a and b). Various inhibitors of ATP-dependent efflux transporters for which etoposide is reported to be a substrate were used to screen for the transporter that had the greatest influence on the etoposide efflux across olfactory and respiratory mucosae. Etoposide efflux across both mucosae was inhibited by 2,4-DNP and quinidine, but not by MK571 or methotrexate. These results demonstrate that the efflux of etoposide across the olfactory and respiratory mucosae is primarily mediated by P-gp. Other investigators have also demonstrated that the efflux of etoposide is primarily mediated by P-gp, whereas other efflux transporters such as MRPs (MRP1 and MPR3) and BCRP play a much less significant role (26,40).

In the presence of 2,4-DNP and quinidine, etoposide transport would be expected to be due to passive diffusion, and the efflux ratio should approach 1.0. Interestingly, the efflux ratios for etoposide in the presence of either 2,4-DNP or quinidine were significantly lower than 1 ($J_{m-s} > J_{s-m}$). This asymmetric passive diffusion across biological membranes has been observed by other researchers (25,41), and is likely a result of the distinct properties of the apical and basolateral domains of each tissue containing different ion channels, additional transport proteins, enzymes, and lipids (42).

The J_{s-m} of etoposide across both the respiratory and olfactory mucosae was found to be concentration-dependent and saturable (Fig. 2), which further supports the existence of efflux transport. The K_m (260.5 μM) and V_{max} (0.179 μM/cm^2 min) values for etoposide efflux in the olfactory mucosa were found to be higher than in the respiratory mucosa (K_m = 46.9 μM and V_{max} = 0.034 μM/cm^2 min). The higher K_m and V_{max} values of etoposide efflux in the olfactory mucosa may be related to the higher expression of P-gp in the olfactory epithelium as demonstrated by the greater staining density observed in the olfactory epithelium (Fig. 1a and b). Other investigators have also reported regional differences in P-gp distribution resulting in differential efflux kinetics (43,44). For example, Stephens *et al.* (44) reported that the net transport ($J_{s-m}-J_{m-s}$) of paclitaxel and digoxin across the murine ileum was greater than across the proximal colon. This coincided with the greater expression of P-gp in the ileum. Tang *et al.* (45) reported that the K_m (252.8 μM) and V_{max} (2.43 pM/cm^2 s) values for [^{3}H]vinblastine efflux across Madin–Darby canine kidney (MDCK) cells that express the human multidrug resistance (MDR1) gene were substantially higher than for efflux across wild-type Madin–Darby canine kidney cells (MDCK-WT) (K_m = 24.5 μM and V_{max} = 0.42 pM/cm^2 s). The differences in the kinetic parameters were attributed to differences in the expression levels of P-gp isoforms, which were substantially higher in MDCK-MDR1 cells compared to MDCK-WT cells.

In summary, P-gp is localized on the apical surface of the epithelium and within the submucosal vasculature/lymphatics and the nasal glands of bovine olfactory and respiratory

mucosae, and it is active in effluxing etoposide, a P-gp substrate. Immunohistochemistry demonstrates that the expression of P-gp is higher in the olfactory epithelium compared to the respiratory epithelium. These results help to identify P-gp-mediated efflux as a biological factor that influences direct nose-to-brain transport of solutes along with other reported physicochemical factors (46). Given the recent interest in exploiting the nasal cavity as a portal for delivering drugs to both the CNS and the systemic circulation, the presence of efflux transporters such as P-gp could have a significant impact on the bioavailability (CNS and systemic) of a wide range of structurally diverse substrates.

REFERENCES

1. M. Dahlin, U. Bergman, B. Jansson, E. Bjork, and E. Brittebo. Transfer of dopamine in the olfactory pathway following nasal administration in mice. *Pharm. Res.* **17**:737–742 (2000).

2. T. Sakane, M. Akizuki, M. Yoshida, S. Yamashita, T. Nadai, M. Hashida, and H. Sezaki. Transport of cephalexin to the cerebrospinal fluid directly from the nasal cavity. *J. Pharm. Pharmacol.* **43**:449–451 (1991).

3. T. C. A. Kumar, G. F. X. David, A. Sankaranarayanan, V. Puri, and K. R. Sundram. Pharmacokinetics of progesterone after its administration to ovariectomized rhesus monkeys by injection, infusion, or nasal spraying. *Proc. Natl. Acad. Sci. USA* **79**:4185–4189 (1982).

4. R. J. Henry, N. Ruano, D. Casto, and R. H. Wolf. A pharmacokinetic study of midazolam in dogs: nasal drop *vs.* atomizer administration. *Pediatr. Dent.* **20**:321–326 (1998).

5. W. H. Frey II, J. Liu, X. Chen, R. G. Thorne, J. R. Fawcett, T. A. Ala, and Y.-E. Rahman. Delivery of ^{125}I-NGF to the brain via the olfactory route. *Drug Deliv.* **4**:87–92 (1997).

6. S. S. Erlich, J. G. McComb, S. Hyman, and M. H. Weiss. Ultrastructural morphology of the olfactory pathway for cerebrospinal fluid drainage in the rabbit. *J. Neurosurg.* **64**:466–473 (1986).

7. S. Kida, A. Pantazis, and R. O. Weller. CSF drains directly from the subarachnoid space into nasal lymphatics in the rat. Anatomy, histology and immunological significance. *Neuropathol. Appl. Neurobiol.* **19**:480–488 (1993).

8. R. G. Thorne, C. R. Emory, T. A. Ala, and W. H. Frey II. Quantitative analysis of the olfactory pathway for drug delivery to the brain. *Brain Res.* **692**:278–282 (1995).

9. H. Tjalve, J. Henriksson, J. Tallkvist, B. S. Larsson, and N. G. Lindquist. Uptake of manganese and cadmium from the nasal mucosa into the central nervous system via olfactory pathways in rats. *Pharmacol. Toxicol.* **79**:347–356 (1996).

10. K. Kristensson and Y. Olsson. Retrograde axonal transport of protein. *Brain Res.* **29**:363–365 (1971).

11. K. J. Chou and M. D. Donovan. Distribution of antihistamines into the CSF following intranasal delivery. *Biopharm. Drug Dispos.* **18**:335–346 (1997).

12. H. S. Chow, Z. Chen, and G. T. Matsuura. Direct transport of cocaine from the nasal cavity to the brain following intranasal cocaine administration in rats. *J. Pharm. Sci.* **88**:754–758 (1999).

13. X.-Q. Chen, J. R. Fawcett, Y.-E. Rahman, T. A. Ala, and W. H. Frey II. Delivery of nerve growth factor to the brain via the olfactory pathway. *J. Alzheimer's Dis.* **1**:35–44 (1998).

14. F. Thiebaut, T. Tsuruo, H. Hamada, M. M. Gottesman, I. Pastan, and M. C. Willingham. Cellular localization of the multidrug-resistance gene product P-glycoprotein in normal human tissues. *Proc. Natl. Acad. Sci. USA* **84**:7735–7738 (1987).

15. H. Sun, H. Dai, N. Shaik, and W. F. Elmquist. Drug efflux transporters in the CNS. *Adv. Drug Deliv. Rev.* **55**:83–105 (2003).

16. A. H. Dantzig, R. L. Shepard, J. Cao, K. L. Law, W. J. Ehlhardt, T. M. Baughman, T. F. Bumol, and J. J. Starling. Reversal of P-glycoprotein-mediated multidrug resistance by a potent cyclopropyldibenzosuberane modulator, LY335979. *Cancer Res.* **56**:4171–4179 (1996).

17. A. H. Schinkel and J. W. Jonker. Mammalian drug efflux transporters of the ATP binding cassette (ABC) family: an overview. *Adv. Drug Deliv. Rev.* **55**:3–29 (2003).

18. C. F. Higgins and M. M. Gottesman. Is the multidrug transporter a flippase? *Trends Biochem. Sci.* **17**:18–21 (1992).

19. M. A. Wioland, J. Fleury-Feith, P. Corlieu, F. Commo, G. Monceaux, J. Lacau-St-Guily, and J. F. Bernaudin. CFTR, MDR1, and MRP1 immunolocalization in normal human nasal respiratory mucosa. *J. Histochem. Cytochem.* **48**:1215–1222 (2000).

20. C. L. Graff and G. M. Pollack. P-glycoprotein attenuates brain uptake of substrates after nasal instillation. *Pharm. Res.* **20**:1225–1230 (2003).

21. C. L. Graff and G. M. Pollack. Functional evidence for P-glycoprotein at the nose–brain barrier. *Pharm. Res.* **22**:86–93 (2005).

22. K. K. Kandimalla and M. D. Donovan. Carrier mediated transport of chlorpheniramine and chlorcyclizine across bovine olfactory mucosa: implications on nose-to-brain transport. *J. Pharm. Sci.* **94**:613–624 (2005).

23. L. Campbell, A.-N. G. Abulrob, L. E. Kandalaft, S. Plummer, A. J. Hollins, A. Gibbs, and M. Gumbleton. Constitutive expression of P-glycoprotein in normal lung alveolar epithelium and functionality in primary alveolar epithelial cultures. *J. Pharmacol. Exp. Ther.* **304**:441–452 (2003).

24. V. D. Makhey, A. Guo, D. A. Norris, P. Hu, J. Yan, and P. J. Sinko. Characterization of the regional intestinal kinetics of drug efflux in rat and human intestine and in Caco-2 cells. *Pharm. Res.* **15**:1160–1167 (1998).

25. Y. Emi, D. Tsunashima, K. Ogawara, K. Higaki, and T. Kimura. Role of P-glycoprotein as a secretory mechanism in quinidine absorption from rat small intestine. *J. Pharm. Sci.* **87**:295–299 (1998).

26. K. O. Hamilton, E. Topp, I. Makagiansar, T. Siahaan, M. Yazdanian, and K. L. Audus. Multidrug resistance-associated protein-1 functional activity in Calu-3 cells. *J. Pharmacol. Exp. Ther.* **298**:1199–1205 (2001).

27. R. H. Stephens, C. A. O'Neill, A. Warhurst, G. L. Carlson, M. Rowland, and G. Warhurst. Kinetic profiling of P-glycoprotein-mediated drug efflux in rat and human intestinal epithelia. *J. Pharmacol. Exp. Ther.* **296**:584–591 (2001).

28. N. Zelcer, T. Saeki, G. Reid, J. H. Beijnen, and P. Borst. Characterization of drug transport by the human multidrug resistance protein 3 (ABCC3). *J. Biol. Chem.* **276**:46400–46407 (2001).

29. F. Thiebaut, T. Tsuruo, H. Hamada, M. M. Gottesman, I. Pastan, and M. C. Willingham. Immunohistochemical localization in normal tissues of different epitopes in the multidrug transport protein P170: evidence for localization in brain capillaries and crossreactivity of one antibody with a muscle protein. *J. Histochem. Cytochem.* **37**:159–164 (1989).

30. Z. S. Chen, K. Lee, S. Walther, R. B. Raftogianis, M. Kuwano, H. Zeng, and G. D. Kruh. Analysis of methotrexate and folate transport by multidrug resistance protein 4 (ABCC4): MRP4 is a component of the methotrexate efflux system. *Cancer Res.* **62**:3144–3150 (2002).

31. J. H. Hooijberg, H. J. Broxterman, M. Kool, Y. G. Assaraf, G. J. Peters, P. Noordhuis, R. J. Scheper, P. Borst, H. M. Pinedo, and G. Jansen. Antifolate resistance mediated by the multidrug resistance proteins MRP1 and MRP2. *Cancer Res.* **59**:2532–2535 (1999).

32. P. Breedveld, N. Zelcer, D. Pluim, O. Sonmezer, M. M. Tibben, J. H. Beijnen, A. H. Schinkel, O. van Tellingen, P. Borst, and J. H. Schellens. Mechanism of the pharmacokinetic interaction between methotrexate and benzimidazoles: potential role for breast cancer resistance protein in clinical drug–drug interactions. *Cancer Res.* **64**:5804–5811 (2004).

33. H. Zeng, L. J. Bain, M. G. Belinsky, and G. D. Kruh. Expression of multidrug resistance protein-3 (multispecific organic anion transporter-D) in human embryonic kidney 293 cells confers resistance to anticancer agents. *Cancer Res.* **59**:5964–5967 (1999).

34. D. R. Adams. Fine structure of the vomeronasal and septal olfactory epithelia and of glandular structures. *Microsc. Res. Tech.* **23**:86–97 (1992).

35. K. K. Kandimalla. Carrier mediated transport of small molecules across bovine nasal mucosa: implications in nose-to-brain transport. Ph.D. thesis, University of Iowa, 2004.

36. B. P. Menco. Qualitative and quantitative freeze-fracture studies on olfactory and nasal respiratory structures of frog, ox, rat, and dog. I. A general survey. *Cell Tissue Res.* **207**:183–209 (1980).

37. M. C. Schmidt, D. Simmen, M. Hilbe, P. Boderke, G. Ditzinger, J. Sandow, S. Lang, W. Rubas, and H. P. Merkle. Validation of excised bovine nasal mucosa as *in vitro* model to study drug transport and metabolic pathways in nasal epithelium. *J. Pharm. Sci.* **89**:396–407 (2000).

38. V. Longo, A. Mazzaccaro, F. Naldi, and P. G. Gervasi. Drug-metabolizing enzymes in liver, olfactory, and respiratory epithelium of cattle. *J. Biochem. Toxicol.* **6**:123–128 (1991).

39. P. Larsson, H. Pettersson, and H. Tjalve. Metabolism of aflatoxin B1 in the bovine olfactory mucosa. *Carcinogenesis* **10**:1113–1118 (1989).

40. J. D. Allen, S. C. van Dort, M. Buitelaar, O. van Tellingen, and A. H. Schinkel. Mouse breast cancer resistance protein (Bcrp1/Abcg2) mediates etoposide resistance and transport, but etoposide oral availability is limited primarily by P-glycoprotein. *Cancer Res.* **63**:1339–1344 (2003).

41. A. Collett, N. B. Higgs, E. Sims, M. Rowland, and G. Warhurst. Modulation of the permeability of H2 receptor antagonists cimetidine and ranitidine by P-glycoprotein in rat intestine and the human colonic cell line Caco-2. *J. Pharmacol. Exp. Ther.* **288**:171–178 (1999).

42. E. M. Fish and B. A. Molitoris. Alterations in epithelial polarity and the pathogenesis of disease states. *N. Engl. J. Med.* **330**:1580–1588 (1994).

43. J. Kunta, J. Yan, V. D. Makhey, and P. J. Sinko. Active efflux kinetics of etoposide from rabbit small intestine and colon. *Biopharm. Drug Dispos.* **21**:83–93 (2000).

44. R. H. Stephens, J. Tanianis-Hughes, N. B. Higgs, M. Humphrey, and G. Warhurst. Region-dependent modulation of intestinal permeability by drug efflux transporters: *in vitro* studies in mdr1a(−/−) mouse intestine. *J. Pharmacol. Exp. Ther.* **303**:1095–1101 (2002).

45. F. X. Tang, K. Horie, and R. T. Borchardt. Are MDCK cells transfected with the human MDR1 gene a good model of the human intestinal mucosa? *Pharm. Res.* **19**:765–772 (2002).

46. L. Illum. Transport of drugs from the nasal cavity to the central nervous system. *Eur. J. Pharm. Sci.* **11**:1–18 (2000).